

# Activation of the integrated stress response during T helper cell differentiation

Stefanie Scheu<sup>1,2,5</sup>, Daniel B Stetson<sup>1,2,5</sup>, R Lee Reinhardt<sup>1,2</sup>, Jess H Leber<sup>1,3</sup>, Markus Mohrs<sup>4</sup> & Richard M Locksley<sup>1,2</sup>

Adaptive immune responses require clonal expansion and differentiation of naive T cells into cytokine-secreting effector cells. After priming via signals through the T cell receptor, naive T helper cells express cytokine mRNA but do not secrete cytokine protein without additional T cell receptor stimulation. Here we show that primed T cells demonstrated phosphorylation of eukaryotic initiation factor 2- $\alpha$  (eIF2 $\alpha$ ), a 'collapsed' polysome profile, increased expression of stress-response genes and accumulation of cytoplasmic granules associated with RNA-binding proteins, all features of the integrated stress response. Restimulation of the cells resulted in rapid eIF2 $\alpha$  dephosphorylation, ribosomal mRNA loading and cytokine secretion. Interference with the function of granule-associated proteins or accumulation of phosphorylated eIF2 $\alpha$  enhanced release of interleukin 4 during T helper type 2 priming. Therefore, T lymphocytes require components of the integrated stress response to uncouple differentiation from the execution of effector functions.

T lymphocytes mediate adaptive immunity by differentiating from naive, quiescent precursors into cytokine-secreting effector cells. At present, models suggest both temporal and spatial separation of CD4<sup>+</sup> helper T cell differentiation and effector function. At the onset of an infection, dendritic cells carry antigens and information regarding the nature of the pathogen from the site of infection to secondary lymphoid tissues, where they direct the clonal expansion and differentiation of naive T cells over many hours<sup>1</sup>. Differentiated effector T cells then migrate into adjacent B cell follicles or exit the secondary lymphoid tissues for peripheral sites of infection, where their cytokines are produced in abundance after re-encountering antigen to mediate help for B cells or activation of myeloid cells.

*In vitro*, effector cytokines such as interleukin 4 (IL-4) and interferon- $\gamma$  (IFN- $\gamma$ ) are poorly detected after initial priming of naive T cells but are abundantly secreted after a second T cell receptor (TCR) stimulation. Those observations are thought to reflect the need for chromatin alterations necessary to decondense the cytokine genomic loci to establish their accessibility<sup>2</sup>. Transcription is initiated at cytokine loci within hours of priming<sup>3</sup>, however, leaving it unclear why the proteins are not detected. In an attempt to track cytokine-producing cells by a more sensitive method, bicistronic IL-4 and IFN- $\gamma$  reporter mice, called '4get' (IL-4 green fluorescent protein (GFP)-enhanced transcript) and 'Yeti' (yellow fluorescent protein-enhanced transcript for IFN- $\gamma$ ), respectively, have been generated. These mice contain bicistronic cytokine 'knock-in' genes linked by an internal ribosomal entry site (IRES) with downstream fluorescent marker genes that, when translated into protein, 'tag' cells that are

signaled to express IL-4 or IFN- $\gamma$  with green or yellow intracellular fluorescent protein, respectively<sup>4,5</sup>.

The integrated stress response (ISR), a general stress-response program conserved from yeast to mammals, is known to modulate protein biosynthesis by integrating various types of stress signals, including endoplasmic reticulum stress, amino acid deprivation, infection with double-stranded RNA viruses, heme deficiency and oxidative stress<sup>6-9</sup>. Those diverse signals activate specific stress kinases, each of which converges on the phosphorylation of serine 51 of the  $\alpha$ -subunit of eukaryotic initiation factor 2 (eIF2), which has GTPase activity. That modification alters the capacity of eIF2 $\alpha$  to be 'recharged' by the nucleotide-exchange factor eIF2B, which subsequently leads to a decrease in the availability of active initiation complexes and thus attenuates translation. At the same time, depending on the type of initiating stress and the cells involved, activation of the ISR also mobilizes stress-induced gene expression involved in cell growth and differentiation<sup>10</sup>. Defects in the ISR are associated with the development of several important pathologies, including diabetes, Alzheimer disease and viral infection<sup>11-13</sup>. Here, we report a previously undescribed mechanism of effector cytokine production by a pathway that shares many features with the ISR.

## RESULTS

### Uncoupled production of cytokine mRNA and protein

When we primed naive CD4<sup>+</sup> T cells from 4get, Yeti or wild-type mice with complexes of peptide and major histocompatibility complex in T helper type 1 (T<sub>H</sub>1)- or T<sub>H</sub>2-polarizing conditions, we detected

<sup>1</sup>Howard Hughes Medical Institute, <sup>2</sup>Department of Medicine and Department of Microbiology & Immunology, and <sup>3</sup>Department of Biochemistry and Biophysics, University of California San Francisco, San Francisco, California 94143, USA. <sup>4</sup>Trudeau Institute, Saranac Lake, New York 12983, USA. <sup>5</sup>These authors contributed equally to this work. Correspondence should be addressed to R.M.L. (locksley@medicine.ucsf.edu).

Received 4 August 2005; accepted 25 March 2006; published online 7 May 2006; doi:10.1038/ni1338

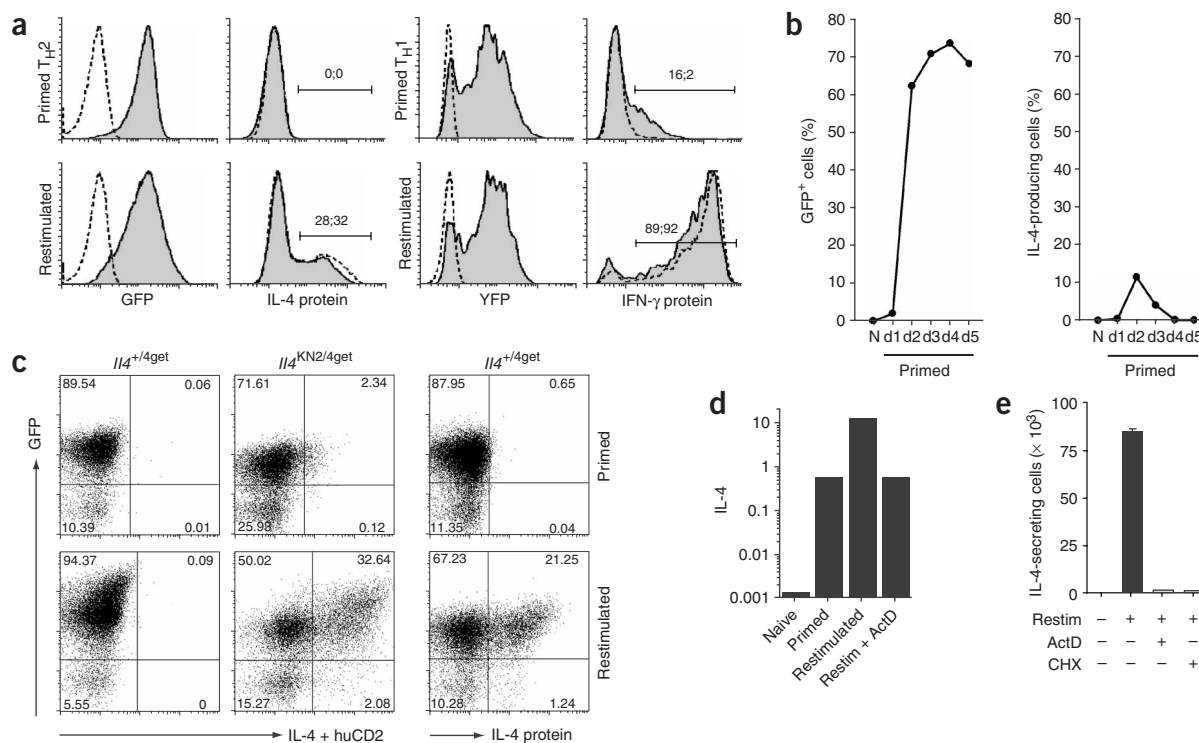


**Figure 1** Cytokine mRNA and protein expression are dissociated in primed  $T_H2$  cells from IL-4 (4get) and IFN- $\gamma$  (Yeti) reporter mice. **(a)** Flow cytometry for GFP or YFP expression and intracellular IL-4 or IFN- $\gamma$  protein (horizontal axes) in DO11.10 4get (left four histograms) or DO11.10 Yeti (right four histograms) T cells (shaded histograms) and DO11.10 T cells (dashed lines) stimulated for 6 d in  $T_H2$  conditions (left four histograms) or  $T_H1$  conditions (right four histograms) with complexes of peptide and major histocompatibility complex, before (top) and after (bottom) restimulation. Bracketed lines indicate positive gates; numbers above correspond to percentage of 4get or Yeti cells (first number) or plain DO11.10 cells (second number) in the gates. **(b)** Percentage of cells expressing GFP (left) and secreting IL-4 protein (right; capture assay) for 4get  $CD4^+$  T cells stimulated for 5 d in  $T_H2$  conditions with irradiated antigen-presenting cells plus anti-TCR $\beta$  and anti-CD28, assessed during the priming period. **(c)** GFP expression and surface human CD2 (huCD2; left four dot plots) and IL-4 protein (right two dot plots; capture assay) of 4get and 4get KN2  $CD4^+$  T cells on day 5 of the  $T_H2$  priming phase (as in **b**), analyzed before (top) and after (bottom) restimulation. Numbers in quadrants indicate percent cells in each. **(d)** Quantitative RT-PCR for IL-4 expression (normalized to expression of hypoxanthine guanine phosphoribosyl transferase) of DO11.10 T cells that were naive, primed, restimulated, or restimulated and treated with actinomycin D (Restim + ActD). **(e)** ELISPOT assay for IL-4 in primed or primed and restimulated (Restim) DO11.10  $T_H2$  cells with or without actinomycin D (ActD) or cycloheximide (CHX). Number of IL-4-producing cells are presented as mean + s.d. Data are representative of three to seven experiments for each set of conditions.

little IL-4 or IFN- $\gamma$  by intracellular protein staining. Unexpectedly, however, most naive  $CD4^+$  T cells from reporter mice became fluorescent during priming in the respective conditions, starting as early as the second day of the priming culture (**Fig. 1a,b**). In accordance with previous studies, TCR restimulation resulted in rapid cytokine protein production, and IFN- $\gamma$  was secreted from more primed  $T_H1$  cells than was IL-4 from primed  $T_H2$  cells<sup>14</sup>. Kinetic analysis using a sensitive cytokine capture assay demonstrated IL-4 protein from a small number of  $T_H2$  primed cells on day 2 when cells became GFP<sup>+</sup>, but protein production ceased as cell division began, and it became undetectable by day 4 (**Fig. 1b** and data not shown). In contrast, primed T cells remained GFP<sup>+</sup> up to 8 d, although the GFP decayed with a half-life of 18 h in the presence of translation inhibitors *in vitro*, consistent with its ongoing translation (data not shown). To support that observation, we adoptively transferred  $T_H2$ -primed, GFP<sup>+</sup> DO11.10 4get  $CD4^+$  T cells into recipient BALB/c mice. After 5–7 weeks, approximately 70% of DO11.10 T cells recovered from the spleen remained GFP<sup>+</sup>, whereas comparably ‘parked’ naive, DO11.10 4get  $CD4^+$  T cells that were GFP<sup>-</sup> before transfer remained GFP<sup>-</sup> over similar periods. Although none of the recovered DO11.10 cells generated IL-4 protein spontaneously, as assessed by enzyme-linked immunosorbent assay (ELISA) or enzyme-linked immunospot

(ELISPOT) assay, the GFP<sup>+</sup> cells produced IL-4 rapidly after stimulation, whereas the GFP<sup>-</sup> cells produced only small amounts of IL-4 and after substantial delay (**Supplementary Fig. 1** online). To rule out the possibility that those results reflected limited sensitivity of the antibodies to IL-4, we used mice containing a human *CD2* reporter gene ‘knocked into’ *Il4* on one allele<sup>15</sup> and the IL-4–IRES–GFP reporter cassette on the other allele. When we stimulated T cells from these mice in the same conditions as above, detection of CD2 precisely mirrored the detection of IL-4 protein, as assessed by intracellular cytokine staining. Although both primed and restimulated cells were GFP<sup>+</sup>, only restimulated cells had high expression of surface CD2 and IL-4 protein (**Fig. 1c**). The high expression of IL-4 and CD2, despite the positioning of genes on separate alleles, is consistent with the predominance of biallelic activation of both IL-4 chromosomal loci during  $CD4^+$  T cell priming, as noted before<sup>4</sup>. Because apoptosis complicates the further analysis of cells stimulated in  $T_H1$  conditions<sup>16</sup>, we did additional studies in  $T_H2$  conditions to explore the mechanisms that result in attenuation of IL-4 translation during T cell priming.

We used quantitative RT-PCR to measure IL-4 transcripts during the differentiation of  $T_H2$  cells; we evaluated only spliced and polyadenylated IL-4 transcripts, as we used oligo(dT) to prime the reverse

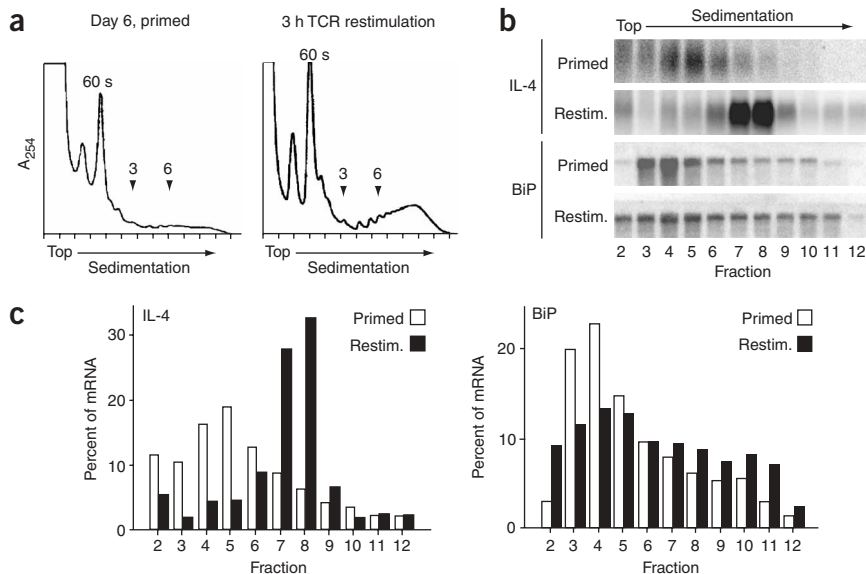


**Figure 2** Polysome analysis of primed and restimulated  $T_H2$  cells. **(a)** Representative polysome profiles of primed DO11.10  $T_H2$  cells (left) and DO11.10  $T_H2$  cells restimulated for 3 h with plate-bound complexes of I-A<sup>d</sup> and ovalbumin peptide (amino acids 247–265; right). 60s, peak corresponding to the 60s large ribosomal subunit; downward arrows (3,6) indicate peaks corresponding to three and six ribosomes. Data are from one of four representative experiments. **(b)** Representative RNA blots for *IL4* or *Hspa5* (BiP) mRNA in fractions 2–12 collected from polysome gradients of primed and restimulated (Restim.)  $T_H2$  cells (fraction numbers below lanes) correspond to hash marks along the horizontal axes of **a**. **(c)** Densitometric quantification of the relative RNA blot signal intensities across the gradient for *IL4* transcripts (left) or *Hspa5* transcripts (BiP; right).

transcription reaction and primers spanning exon junctions in the PCR assays. IL-4 transcripts in primed cells increased about 1,000-fold compared with those in naive T cells, whereas IL-4 protein was undetectable without restimulation (**Fig. 1d,e**). After restimulation, IL-4 transcripts increased 30- to 100-fold further, whereas the number of protein-producing cells increased more than 1,000-fold (**Fig. 1d,e**). The increase in IL-4 transcripts after restimulation of wild-type cells was accompanied by an enhanced mean fluorescence intensity of GFP from the 4get cells after restimulation, demonstrating that the GFP fluorescence was not already saturated in primed cells (**Fig. 1c,d**). The transcriptional inhibitor actinomycin D ablated transcripts induced by restimulation but not the amount of primed mRNA, and inhibition of transcription (with actinomycin D) or translation (with cycloheximide) blocked IL-4 protein production (**Fig. 1e**).

### Translation efficiency in primed and restimulated $T_H2$ cells

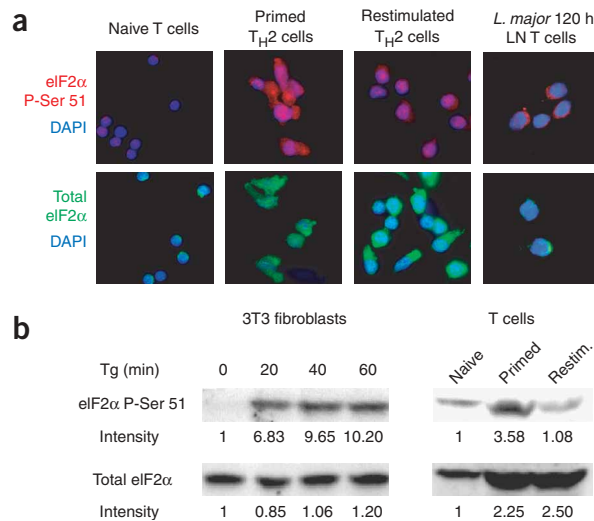
One explanation for the discordance in IL-4 and GFP protein expression in the reporter cells is that translation of GFP is potentiated (over that of IL-4) by the IRES in the reporter allele<sup>4</sup>. IRES elements confer translational competency during periods of translational arrest<sup>17</sup> and are ‘preferentially’ active during cell division<sup>18</sup>. To assess the global translation activity in wild-type cells, as reflected by the amount of ribosomes loaded onto mRNAs, we compared the total cellular polysome profiles of primed naive T cells with those of restimulated  $T_H2$  cells. The polysome profile of primed (but not restimulated)  $T_H2$  cells was consistent with global translation attenuation, with abundant free ribosomal subunits and a paucity of poly-

some-bound mRNAs (**Fig. 2a**); control cells, including Jurkat T cells and NIH 3T3 fibroblasts, had polysome profiles consistent with active translation (data not shown). Restimulation of primed  $T_H2$  cells, however, caused rapid recovery of a polysome profile consistent with active translation and was coincident with the appearance of IL-4 protein (**Fig. 1a,c**).

We next determined the position of IL-4 transcripts across fractions of a continuous sucrose gradient of polysomes from primed and restimulated  $T_H2$  cells. In primed cells, which produce little IL-4 protein, IL-4 transcripts were present at the top of the gradient, reflecting inefficient association with the dense ribosomal machinery (**Fig. 2b**). In contrast, IL-4 transcripts from restimulated cells were present in fractions corresponding to the density of loading by six to seven ribosomes (**Fig. 2b,c**), which is consistent with optimal translation, given that IL-4 mRNA is about 500 nucleotides in length and has a ribosomal spacing of 1 every approximately 80 nucleotides. However, not all cellular transcripts were present in the same gradient fractions: we recovered mRNA encoding BiP, an endoplasmic reticulum chaperone, from higher fractions of the gradient in both primed

### Figure 3 Increased phosphorylation of eIF2 $\alpha$ serine 51 in $T_H2$ cells after priming.

**(a)** Microscopy of naive CD4<sup>+</sup> T cells, primed and restimulated  $T_H2$  cells and  $T_H2$  cells sorted from draining lymph nodes of *L. major*-infected mice (far right), stained for eIF2 $\alpha$  phosphorylated at serine 51 (eIF2 $\alpha$  P-Ser 51; top; red) or total eIF2 $\alpha$  (bottom; green). Nuclei are blue (DAPI). Original magnification,  $\times 400$ . **(b)** Immunoblot for eIF2 $\alpha$  phosphorylated at serine 51 (top) or total eIF2 $\alpha$  (bottom) in lysates from equal numbers of NIH 3T3 cells treated for various times (above lanes) with 0.4  $\mu$ M thapsigargin (Tg; left) and in lysates from equal numbers of naive, primed or restimulated  $T_H2$  cells (right). Numbers below lanes indicate intensity relative to that of unstimulated 3T3 fibroblasts or naive T cells. Data are from one of three representative experiments.



and restimulated cells, indicating comparable association with ribosomes in both conditions (Fig. 2b,c). The endogenous BiP mRNA, similar to the 'knock-in' cytokine transcripts in the reporter mice, contains an IRES<sup>19</sup>. These data suggest that naive CD4<sup>+</sup> T cells primed by TCR engagement are initially restricted in cytokine translation that is then 'released' after TCR re-engagement.

### Phosphorylation of eIF2 $\alpha$ in primed and restimulated T<sub>H</sub>2 cells

An important checkpoint in the eukaryotic translation initiation process is the availability of a charged ternary complex, consisting of eIF2 bound to GTP and the methionyl-initiator tRNA. This ternary complex delivers the charged methionyl-initiator tRNA to small ribosomal subunit-mRNA complexes. Energy for eIF2 activity is

generated by hydrolysis of its associated GTP by eIF5, and the resulting eIF2-GDP complex is recharged by the exchange factor eIF2B, allowing eIF2 to recycle<sup>20</sup>. In the presence of cell stress, eIF2 is phosphorylated at serine 51 of its  $\alpha$ -subunit, abolishing its capacity to be recharged by eIF2B and hence attenuating translation. To assess possible involvement of eIF2 $\alpha$  phosphorylation in the observed translational arrest, we compared immunofluorescence staining of total and phosphorylated eIF2 $\alpha$  (phospho-eIF2 $\alpha$ ) in naive T cells and primed and restimulated T<sub>H</sub>2 cells. In contrast to naive cells, which contained little phospho-eIF2 $\alpha$ , primed T<sub>H</sub>2 cells stained uniformly with an antibody specific to phospho-eIF2 $\alpha$ . The intensity of phospho-eIF2 $\alpha$  staining was much less after restimulation, whereas it remained stable for total eIF2 $\alpha$  (Fig. 3a). To assess the *in vivo* relevance

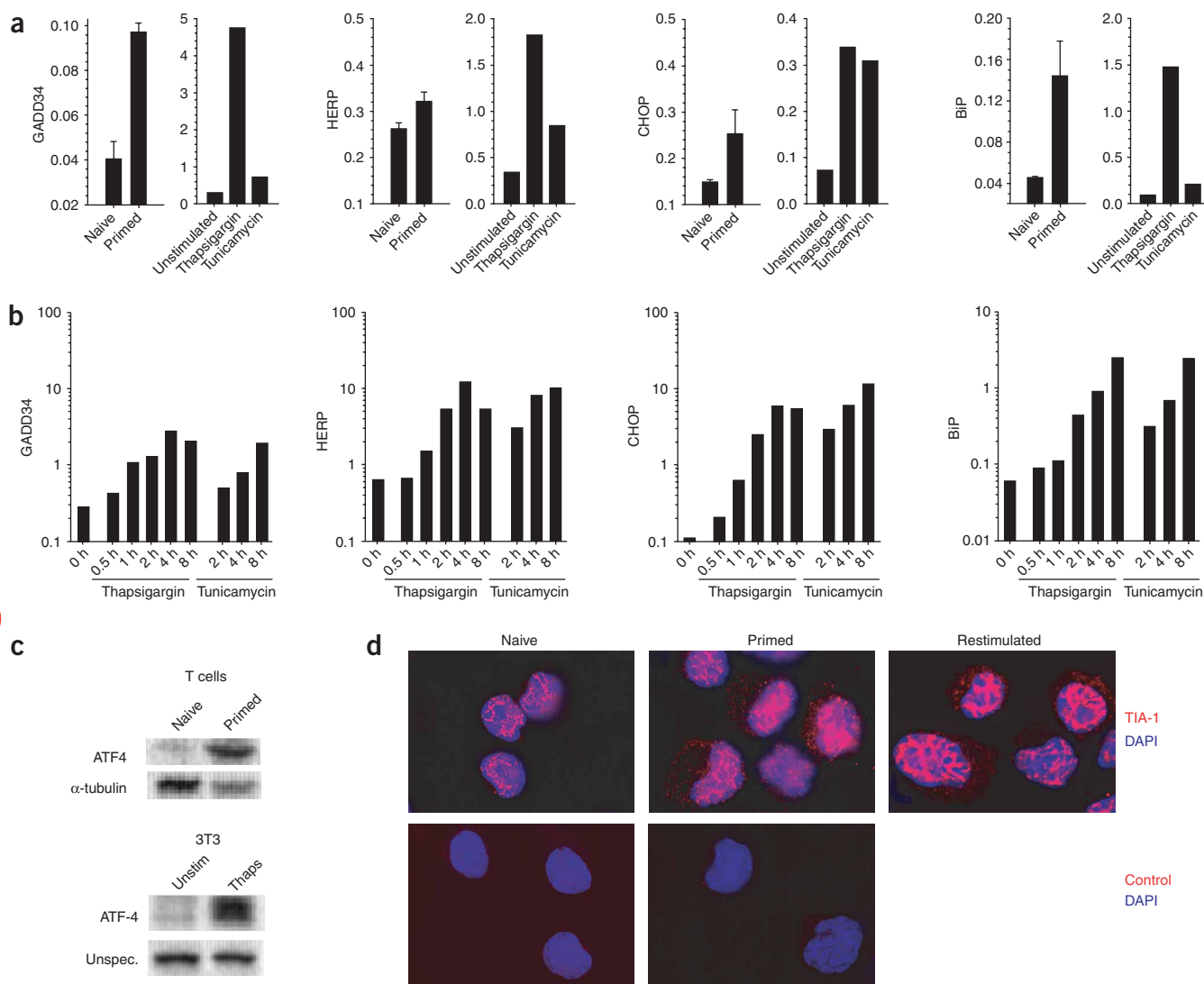


**Figure 4** Expression of stress response-induced genes and the presence of TIA-1-associated granules in naive and T<sub>H</sub>2-primed CD4<sup>+</sup> T cells. **(a)** Quantitative RT-PCR for expression of GADD34, HERP, CHOP and BiP (normalized to expression of hypoxanthine guanine phosphoribosyl transferase) in naive and T<sub>H</sub>2-primed T cells or naive T cells treated for 4 h with 0.1  $\mu$ M thapsigargin or 2  $\mu$ g/ml of tunicamycin. Results are presented as means + s.e.m. or are one representative of two comparable experiments. **(b)** Quantitative RT-PCR, as described in **a**, of NIH 3T3 cells treated with 0.1  $\mu$ M thapsigargin or 2  $\mu$ g/ml of tunicamycin for various times (horizontal axes). Data are one representative of two experiments. **(c)** Immunoblot for ATF4 in lysates (15  $\mu$ g protein per lane) from naive and primed T<sub>H</sub>2 cells (top) and lysates from NIH 3T3 cells left unstimulated (Unstim) or treated for 3 h with 0.1  $\mu$ M thapsigargin (Thaps; bottom). Lower blots,  $\alpha$ -tubulin or a nonspecific band (Nonspec) from blotting for ATF4 serves as a loading control. Data are from one of two representative experiments. **(d)** Immunofluorescence of TIA-1 (red) in naive, T<sub>H</sub>2-primed and restimulated CD4<sup>+</sup> T cells. DAPI nuclear fluorescence is blue. Control, secondary antibody alone. Original magnification,  $\times 1,000$ . Staining is representative of six independent experiments.

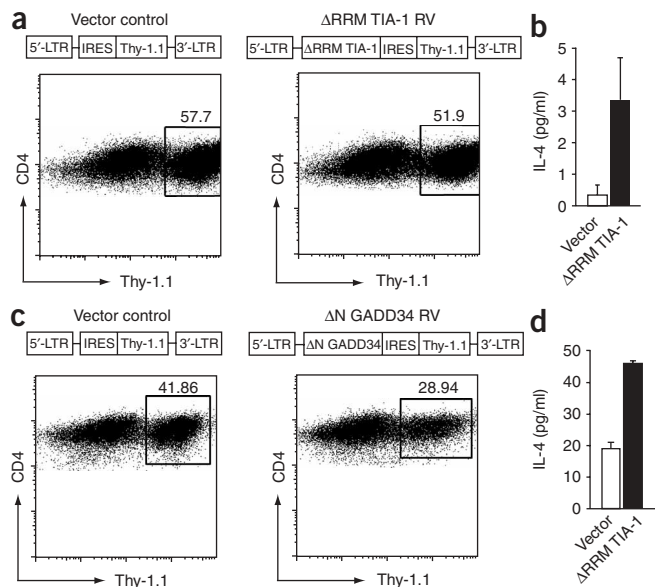


**Figure 5** Expression of dominant negative TIA-1 or constitutively active GADD34 in T cells during  $T_H2$  priming potentiates IL-4 secretion. Naive  $CD4^+$  T cells were infected with empty vector (Vector control) or  $\Delta$ RRM TIA-1 RV (a,b) or  $\Delta$ N GADD34 RV (c,d). (a,c) Flow cytometry of  $T_H2$ -primed cells sorted for CD4 and Thy-1.1 expression after 5 d. Numbers beside boxed areas indicate percent  $CD4^+Thy-1.1^+$  cells. (b,d) IL-4 in supernatants of sorted cells incubated for 48 h without further stimulation in fresh media.  $P < 0.06$  (b) or  $P < 0.05$  (d). Data are one of four representative experiments; error bars represent mean + s.d.

of those findings, we sorted primed  $T_H2$  cells from the draining lymph nodes of mice infected with *Leishmania major*; these parasites stimulate a robust  $T_H2$  response that peaks between 96 and 120 h after infection<sup>21</sup>. The primed  $CD4^+$  T cells had more phospho-eIF2 $\alpha$  than did naive T cells, suggesting that the translation inhibition we noted *in vitro* occurs *in vivo* during clonal expansion in lymph nodes (Fig. 3a).

We confirmed the immunofluorescence microscopy findings by immunoblot analysis of lysates from naive and primed  $T_H2$  cells (Fig. 3b). As a control, lysates from NIH 3T3 fibroblasts showed a substantial increase in eIF2 $\alpha$  phosphorylation after treatment of cells with thapsigargin, a potent inducer of oxidative cell stress. In accordance with the immunofluorescence staining results, there was more total and phospho-eIF2 $\alpha$  in primed  $T_H2$  cells than in naive T cells. Densitometric quantification showed a 1.6-fold increase in the ratio of phospho-eIF2 $\alpha$  to total eIF2 $\alpha$  in primed cells. TCR restimulation, which led to restoration of the polysome profile and the production of IL-4 protein, was associated with rapid dephosphorylation of eIF2 $\alpha$ .

At least four kinases, activated by different types of cell stress, mediate the phosphorylation of eIF2 $\alpha$ : PERK, an endoplasmic reticulum-resident kinase activated by unfolded proteins; GCN2, which couples amino acid availability to translation rates and has been linked to  $CD8^+$  T cell anergy<sup>22</sup>; the double-stranded RNA-dependent kinase PKR, which attenuates translation in response to viral infection; and, in erythroid cells, heme-regulated kinase (HRI), which balances heme availability with globin synthesis<sup>10</sup>. Mutational analysis has suggested that some of these eIF2 $\alpha$  kinases overlap the binding 'footprint' of the guanine nucleotide-exchange factor eIF2B<sup>23</sup>. Attempts to block eIF2 $\alpha$  phosphorylation by retroviral introduction of dominant negative PERK or GCN2 kinases into T cells during

priming led to the death of all transduced cells (Supplementary Fig. 2 online). Retroviral expression of dominant negative IRE1- $\beta$ , which inhibits the endoplasmic reticulum-resident stress kinases IRE1- $\alpha$  and IRE1- $\beta$ , which have a different substrate than eIF2 $\alpha$ <sup>24</sup>, did not affect T cell viability, however, and none of these kinase mutants affected viability when introduced into 3T3 fibroblasts. This suggests that the observed effects were related to the status of eIF2 $\alpha$  phosphorylation.

### Induction of a stress-response phenotype after $T_H2$ cell priming

Although phosphorylation of eIF2 $\alpha$  causes overall attenuation of translation, a subset of specific mRNAs are 'preferentially' translated in those conditions. They include transcription factors such as ATF4, which activate genes required for adaptation and survival during stress, including *Ppp1r15a* (GADD34), *Ddit3* (CHOP), *Herpud1* (Herp) and *Hspa5* (BiP)<sup>6,25–27</sup>. As assessed by immunoblot analysis for ATF4 and quantitative RT-PCR for ATF4 target genes, ATF4 protein and each of the target gene transcripts were more abundant in primed T cells than in naive T cells, consistent with activation of the ISR (Fig. 4). Induction of the ISR pathway in T cells was demonstrated by stimulation of T cells with the known ISR inducers thapsigargin and tunicamycin (Fig. 4a). Of note, transcriptional activation of these genes during T cell differentiation was less than their activation induced by classical but nonphysiological activators of the cell stress response, such as thapsigargin or tunicamycin (Fig. 4a–c).

We next did microarray experiments to determine the relative changes in polysome-associated mRNA in effector T cells. We compared polysome-associated mRNA pooled from fractions 7–12 of sucrose gradients from primed and restimulated cells to evaluate apparent global changes in translation efficiency. We labeled cDNA and hybridized it to an oligonucleotide array complementary to about 17,000 unique mouse transcripts. After restimulation, approximately 700 mRNAs increased more than threefold and about 1,900 transcripts increased more than twofold in polysome association, whereas about 350 transcripts decreased less than 30% and about 1,100 decreased less than 50% (a list of selected genes with known involvement in the ISR or those containing a known IRES is provided in Supplementary Table 1 online). Of note, the stress-response genes *Atf4*, *Ppp1r15a*, *Ddit3*, *Herpud1* and *Hspa5* analyzed above showed either downregulation or only minimal upregulation in their association with polysomes after restimulation, with high signal intensities ( $A > 9$ ) in at least one of two independent experiments, consistent with a relatively high translational efficiency in primed cells (in accordance with Fig. 4a,c). Additional genes known to contain an IRES had an analogous pattern of translational efficiency, including *Nap1l1* and *Vim* (vimentin)<sup>18</sup>, *Oaz1* (ornithine decarboxylase 1)<sup>28</sup>, *Lck*<sup>29</sup>, *Grp58* and *Hsp70* (ref. 30). Transcripts with a strong shift toward the polysomal fraction after restimulation included transcripts encoding  $T_H2$  effector proteins such as IL-4, IL-10 and IL-13 (Supplementary Table 1).

Studies have suggested that members of the RNA-recognition-motif (RRM) family of RNA-binding proteins, TIA-1 and TIAR, associate with untranslated mRNA in discrete cytosolic microdomains during the ISR<sup>31,32</sup>. The presence of phospho-eIF2 $\alpha$  is sufficient to induce aggregation of these nuclear-cytoplasmic-shuttling RRM proteins with stalled initiation complexes<sup>31</sup>. In accordance with that, primed but not naive  $CD4^+$  T cells contained TIA-1-associated cytoplasmic accumulations in essentially all cells (Fig. 4d). TIAR staining was comparable to TIA-1 staining (data not shown). TIA-1-associated granules did not dissipate immediately after restimulation during the period in which IL-4 was secreted (Fig. 4d).

### Influence of TIA-1 and GADD34 activity on the release of IL-4

Expression of a truncated version of TIA-1 lacking the N-terminal RNA-binding domains ( $\Delta$ RRM TIA-1) prevents the formation of stress granules by sequestering the endogenous TIA-1 and TIAR and facilitates the increased translation of cotransfected reporter genes<sup>31,33</sup>. To elucidate the functional involvement of TIA-1 and TIAR in suppressing IL-4 translation during  $T_H2$  cell priming, we retrovirally introduced expression of a dominant negative  $\Delta$ RRM TIA-1 into T cells during priming. As assessed by ELISA, the mutant protein induced an increase in IL-4 release during priming without additional T cell restimulation, in contrast to the vector control (Fig. 5a,b).

In the recovery phase of a cellular stress response, the serine-threonine phosphatase PP1 and its nonenzymatic component GADD34 are at least partially responsible for the dephosphorylation of eIF2 $\alpha$  and 'release' of the translational block. As demonstrated before, expression of a constitutively active N-terminal deletion mutant of GADD34 ( $\Delta$ N GADD34) can efficiently dephosphorylate eIF2 $\alpha$  and attenuate the induction of stress-inducible genes<sup>25,34</sup>. Using retroviral transduction, we introduced expression of  $\Delta$ N GADD34 into T cells during  $T_H2$  priming. Similar to  $\Delta$ RRM TIA-1, the mutant GADD34 induced a substantial increase in IL-4 release during priming (Fig. 5c,d). Of note, the IL-4 release occurred in the absence of the additional induction of IL-4 transcription noted after restimulation of the TCR (Fig. 1c).

### DISCUSSION

Our data have shown that primed CD4<sup>+</sup> T cells use components of the ISR during their differentiation into cytokine-secreting effector cells. The ISR denotes the coordinated cellular response to environmental perturbations, which converge on the need to match the biosynthetic capacity of the endoplasmic reticulum with the transcriptional and translational needs of the cell<sup>10</sup>. We speculate that the requirements for differentiation and rapid clonal expansion generate imbalances in nutrients and induce oxidative or endoplasmic reticulum stress, which is sufficient to cause eIF2 $\alpha$  phosphorylation, thus attenuating general translation. Alternatively, TCR priming might activate this pathway in an 'anticipatory' way. Precedent exists for each model<sup>10</sup>. Two of the kinases that phosphorylate eIF2 $\alpha$  (GCN2 and PERK) are expressed in T cells, and attempts to block their activity using dominant negative proteins expressed during priming proved lethal for differentiating cells. Although various components of the ISR, such as the latent endoplasmic reticulum transcriptional factor ATF6 and the endoplasmic reticulum kinase IRE1, use pathways not including eIF2 $\alpha$ , successful activation of the stress response requires eIF2 $\alpha$  phosphorylation, as many crucial ISR target genes are translated more efficiently in such conditions<sup>10</sup>.

Although T cell priming induced increases in both phosphorylated and total eIF2 $\alpha$ , the increase in phospho-eIF2 $\alpha$  was greater. The total amount of eIF2 $\alpha$  in relation to the total amount of eIF2B and other components of the ribosomal machinery ultimately determines the overall effects of phospho-eIF2 $\alpha$  on protein synthesis. However, as we demonstrated by global polysome profile analysis, primed T cells were translationally attenuated, in contrast to restimulated T cells, and the attenuated state correlated with decreased phospho-eIF2 $\alpha$  in restimulated cells. We corroborated those findings by microarray analysis of polysome-associated transcripts from primed and restimulated  $T_H2$  cells, which indicated that twice as many genes were translationally activate after restimulation. The experimental design strengthened those conclusions, as we used equivalent amounts of mRNA from the two culture conditions, and the primed fractions contained substantially fewer polysome-associated transcripts than did the restimulated

fractions. Phosphorylation of eIF2 $\alpha$  is a central checkpoint of the ISR, and increased phospho-eIF2 $\alpha$  in primed T cells is consistent with activation of the ISR in these cells.

As noted before, many mRNAs are paradoxically translated in conditions of general translational attenuation, including transcription factors, kinases, phosphatases and proto-oncogenes that have been linked to diverse differentiation pathways<sup>25,27,35,36</sup>. In yeast, these pathways are critical for adaptation of the organism to environmental alterations<sup>37</sup>. Also, many mammalian genes contain IRES elements<sup>28</sup>, which confer 'preferential' translational activity during cell division<sup>18</sup>, as supported by our observations of the positioning of BiP in the polysome profile and the effective translation of GFP when 'downstream' of an IRES sequence. Evidence has suggested that translation attenuation favors stalling of ribosomes at 'upstream' open reading frames that in turn facilitates mRNA remodeling, formation of an active IRES and translation of the 'downstream' open reading frame<sup>38</sup>. Similar processes underlie reinitiation at alternative 5' open reading frames for other targets of the ISR<sup>27</sup>. Indeed, several transcripts of genes that contain an IRES or 5' open reading frame and are known to be involved in the ISR showed polysomal association in primed  $T_H2$  cells, in contrast to restimulated  $T_H2$  cells. However, not all known mRNAs that contain IRES elements<sup>28</sup> were translated actively during T cell priming, suggesting that specific IRES sequences are differentially regulated in the course of T cell activation. Alternatively, suppression of translation of key inhibitors may also contribute to activation of critical pathways, such as gene expression mediated by transcription factor NF- $\kappa$ B, during T cell priming<sup>39</sup>. Thus, cells activate a distinct genetic program during periods of translational attenuation, and distinct mechanisms exist that facilitate translation of the key proteins involved in this process.

Despite having linked various components of the ISR to T cell priming, we emphasize that our findings are not entirely concordant with descriptions of this pathway generated using traditional agents to induce cell stress *in vitro*, such as thapsigargin and tunicamycin. Indeed, we have shown that transcriptional activation of ISR target genes was lower in primary T cells after priming than in cells treated with these classical, although nonphysiological, stimuli. Cytoplasmic accumulation of the RRM proteins TIA-1 and TIAR was smaller and more dispersed in primary T cells than in tumor cell lines<sup>33</sup>, and the accumulations did not immediately disaggregate during the period of TCR restimulation. The exact nature and function of these cytosolic, RNA-containing microdomains remains unclear, and even the nomenclature describing the microdomains as 'processing bodies' or 'stress granules' remains imprecise<sup>40</sup>. As for the original observation of efficient translation of GFP coinciding with translational repression of IL-4 from the same bicistronic transcript, the actual subcellular localization of the IL-4 transcripts remains debatable because they are potentially subject to dual regulation. One possibility is that the ongoing loading and translocation of ribosomes at the 3' GFP-cistron prevents efficient compartmentalization of the complete message into TIA-1-TIAR-containing granules, as would be the case for the wild-type IL-4 messages. We found that introduction of dominant negative TIA-1 induced IL-4 release during priming from wild-type T cells, which is consistent with functional involvement of TIA-1-TIAR in restricting robust T cell function. Cytosolic structures (granules) have been shown to incorporate nontranslated mRNA in both yeast and mammalian cells, and their formation has been tightly linked to translational attenuation and sites of mRNA decay<sup>40-42</sup>.

Competence for cytokine expression is gained by transcription through the loci required for 'imprinting' of chromatin changes necessary to achieve epigenetic stabilization of cytokine genes<sup>2</sup>. At

the same time, immediate translation of those effector proteins might contribute additional stress to the expanding endoplasmic reticulum during a period of increased need for amino acids and protein-folding capacity. Similar toxicity to antibody-secreting B cells occurs in the absence of XBP-1, a stress-induced transcription factor whose mRNA is processed by the latent luminal kinase IRE1 (refs. 36,43). Translational attenuation avoids the toxic side effects associated with a rapid increase in the endoplasmic reticulum load due to an expanded protein repertoire<sup>10</sup>. After second antigen contact in the periphery or in the follicles, the translational block of T cells is relieved and the appropriate effector functions can be executed. Further studies of T cell differentiation should provide a model system for investigating components of the ISR pathway in this previously unknown physiological function.

## METHODS

**Mice, parasites and flow cytometry.** The 4get, Yeti, DO11.10 4get, DO11.10 *Tcr $\alpha$ <sup>-/-</sup>* and KN2 mice have been described<sup>4,5,15,21,44</sup>. Female mice 5–10 weeks of age were maintained in accordance with institutional guidelines in the specific pathogen-free facility of the University of California San Francisco. Lymphocytes were isolated and stained for flow cytometry and sorting as described<sup>21</sup>. Cells were analyzed and sorted to more than 99% purity using flow cytometry (Mo-Flo; Dako-Cytomation). Passage of *L. major* and infection of mice have been described<sup>21</sup>. Additional methods are in the **Supplementary Methods** online.

**Cytokine and proliferation assays.** Stimulation of naive CD4<sup>+</sup> T cells in T<sub>H</sub>1 and T<sub>H</sub>2 conditions was done as described<sup>3,21</sup>. ELISPOT assay, ELISA, surface staining by antibody-mediated capture and quantitative RT-PCR for cytokine analysis were done as described<sup>3,21,45</sup>.

**Quantitative RT-PCR for stress-induced genes.** Stimulation of naive CD4<sup>+</sup> T cells in T<sub>H</sub>2 conditions was done as described<sup>3,21</sup>. Naive T cells and 3T3 fibroblasts were stimulated with 100 nM thapsigargin (Sigma-Aldrich) or 2  $\mu$ g/ml of tunicamycin (Calbiochem) for 4 h or the times indicated in **Figures 3b** and **4b**. A DNA Engine Opticon 2 thermal cycler with Opticon Monitor 2 Software (Bio-Rad) was used for quantitative RT-PCR. Primers are available in the **Supplementary Methods** online.

**Polysome analysis.** DO11.10 *Tcr $\alpha$ <sup>-/-</sup>* T cells stimulated for 6 d in T<sub>H</sub>2 conditions were centrifuged over Histopaque (Sigma), were washed and were allowed to 'rest' for 20 min at 37 °C in complete media with 0.1 mg/ml of cycloheximide (Sigma) added for the final 10 min. Cells were washed with ice-cold PBS with cycloheximide and were resuspended in polysome extraction buffer. Restimulated cells were activated for 3 h with 10  $\mu$ g/ml of plate-bound complexes of I-A<sup>d</sup> and ovalbumin peptide (amino acids 247–265)<sup>21</sup>, then were washed and resuspended in extraction buffer. Extracts were separated over 10–50% sucrose gradients by ultracentrifugation. For isolation of fractions, 60% sucrose was pumped into the bottom of the tube and the displaced volumes were collected as different fractions with constant monitoring of absorbance at 254 nm. Extracted RNA was analyzed by RNA blot with <sup>32</sup>P-labeled probes specific for *Il4* or *Hspa5* (BiP) sequences. Additional methods are in the **Supplementary Methods** online.

**Immunofluorescence and immunoblot analysis.** DO11.10 4get-primed T<sub>H</sub>2 cells from the draining popliteal lymph nodes of mice infected with *L. major* were sorted and were spun onto coverslips. Stimulation of naive CD4<sup>+</sup> T cells in T<sub>H</sub>2 conditions was done as described<sup>3,21</sup>. Samples were incubated with rabbit antisera to total eIF2 $\alpha$  (Santa Cruz) or to eIF2 $\alpha$  phosphorylated at serine 51 (Biosource) or with goat antiserum to TIA-1 (Santa Cruz) before being washed and then incubated with indocarbocyanine-labeled antibody to goat (anti-goat) for TIA-1 or indocarbocyanine-labeled antisera to rabbit (Jackson Immunoresearch). Coverslips were counterstained with DAPI (4',6-diamidino-2'-phenylindole dihydrochloride; Roche). For immunoblot analysis, 1  $\times$  10<sup>7</sup> T cells were analyzed with antisera to eIF2 $\alpha$  phosphorylated at serine 51 (Cell Signaling Technologies), total eIF2 $\alpha$ , ATF4 or  $\alpha$ -tubulin (Santa Cruz). Bound

antibodies were detected with horseradish peroxidase-conjugated protein A (for phospho-eIF2 $\alpha$  and total eIF2 $\alpha$ ; Biorad) and horseradish peroxidase-conjugated anti-rabbit (for ATF4; Promega) or anti-mouse (for  $\alpha$ -tubulin; Promega) by enhanced chemiluminescence (Amersham). Additional methods are in the **Supplementary Methods** online.

**Retrovirus infection.** The C-terminal fragments of mouse TIA-1 (amino acids 241–386;  $\Delta$ RRM)<sup>31</sup> and mouse GADD34 (amino acids 241–657;  $\Delta$ N)<sup>25</sup> were amplified from mouse spleen cDNA, were confirmed by sequencing and were ligated into MSCV-IRES-Thy-1.1 retroviral vector<sup>46</sup> immediately upstream of the IRES-Thy-1.1 sequence. Retrovirus was produced in the PHOENIX packaging cell line and CD4<sup>+</sup> T cells were transfected as described<sup>47</sup>. After being washed, designated T<sub>H</sub>2 cells were incubated undisturbed in media without cytokines. For experiments using GADD34, 10  $\mu$ g/ml of anti-IL-4 receptor (clone M1; BD Biosciences) was included. Supernatants were collected 48 h later and were analyzed for IL-4 by ELISA with a detection limit of 2 pg/ml (R&D Systems).

**Microarray analysis.** This is described in the **Supplementary Methods** online.

**Accession code.** GEO: microarray data, GSE4500.

*Note: Supplementary information is available on the Nature Immunology website.*

## ACKNOWLEDGMENTS

We thank Z. Wang, C. McArthur, N. Flores, J. Lin, L. Stowring and A. Barczak for technical support; R. Wek, W. Sha, N. Kedersha and P. Anderson for reagents; D. Ron and P. Walter for reagents and discussions; and J. Cyster for comments. Supported by the National Institutes of Health (AI30663 and HL56385 to R.M.L.), Deutsche Forschungsgemeinschaft (SCHE692/1-1 to S.S.), the Juvenile Diabetes Research Foundation-Irvington Institute (R.L.R.) and the Ellison Medical Foundation (R.M.L.).

## COMPETING INTERESTS STATEMENT

The authors declare that they have no competing financial interests.

Published online at <http://www.nature.com/natureimmunology/>

Reprints and permissions information is available online at <http://npg.nature.com/reprintsandpermissions/>

1. Catron, D.M., Itano, A.A., Pape, K.A., Mueller, D.L. & Jenkins, M.K. Visualizing the first 50 hr of the primary immune response to a soluble antigen. *Immunity* **21**, 341–347 (2004).
2. Ansel, K.M., Lee, D.U. & Rao, A. An epigenetic view of helper T cell differentiation. *Nat. Immunol.* **4**, 616–623 (2003).
3. Grogan, J.L. *et al.* Early transcription and silencing of cytokine genes underlie polarization of T helper cell subsets. *Immunity* **14**, 205–215 (2001).
4. Mohr, M., Shinkai, K., Mohr, K. & Locksley, R.M. Analysis of type 2 immunity in vivo with a bicistronic IL-4 reporter. *Immunity* **15**, 303–311 (2001).
5. Stetson, D.B. *et al.* Constitutive cytokine mRNAs mark natural killer (NK) and NK T cells poised for rapid effector function. *J. Exp. Med.* **198**, 1069–1076 (2003).
6. Harding, H.P. *et al.* Regulated translation initiation controls stress-induced gene expression in mammalian cells. *Mol. Cell Biol.* **6**, 1099–1108 (2000).
7. Williams, B.R. PKR; a sentinel kinase for cellular stress. *Oncogene* **18**, 6112–6120 (1999).
8. Lu, L., Han, A.P. & Chen, J.J. Translation initiation control by heme-regulated eukaryotic initiation factor 2 $\alpha$  kinase in erythroid cells under cytoplasmic stresses. *Mol. Cell Biol.* **21**, 7971–7980 (2001).
9. Zhang, P. *et al.* The GCN2 eIF2 $\alpha$  kinase is required for adaptation to amino acid deprivation in mice. *Mol. Cell Biol.* **22**, 6681–6688 (2002).
10. Harding, H.P., Calton, M., Urano, F., Novoa, I. & Ron, D. Transcriptional and translational control in the mammalian unfolded protein response. *Annu. Rev. Cell Dev. Biol.* **18**, 575–599 (2002).
11. Zhang, P. *et al.* The PERK eukaryotic initiation factor 2 $\alpha$  kinase is required for the development of the skeletal system, postnatal growth, and the function and viability of the pancreas. *Mol. Cell Biol.* **22**, 3864–3874 (2002).
12. Chang, R.C., Wong, A.K., Ng, H.K. & Hugon, J. Phosphorylation of eukaryotic initiation factor-2 $\alpha$  (eIF2 $\alpha$ ) is associated with neuronal degeneration in Alzheimer's disease. *Neuroreport* **13**, 2429–2432 (2002).
13. Aridor, M. & Balch, W.E. Integration of endoplasmic reticulum signaling in health and disease. *Nat. Med.* **5**, 745–751 (1999).
14. Openshaw, P. *et al.* Heterogeneity of intracellular cytokine synthesis at the single-cell level in polarized T helper 1 and T helper 2 populations. *J. Exp. Med.* **182**, 1357–1367 (1995).

15. Mohrs, K., Wakil, A.E., Killeen, N., Locksley, R.M. & Mohrs, M.A. Two-step process for cytokine production revealed by IL-4 dual-reporter mice. *Immunity* **23**, 419–429 (2005).
16. Zhang, X. *et al.* Unequal death in T helper cell (Th)1 and Th2 effectors: Th1, but not Th2, effectors undergo rapid Fas/FasL-mediated apoptosis. *J. Exp. Med.* **185**, 1837–1849 (1997).
17. Fernandez, J., Yaman, I., Sarnow, P., Snider, M.D. & Hatzoglou, M. Regulation of internal ribosomal entry site-mediated translation by phosphorylation of the translation initiation factor eIF2 $\alpha$ . *J. Biol. Chem.* **277**, 19198–19205 (2002).
18. Qin, X. & Sarnow, P. Preferential translation of internal ribosome entry site-containing mRNAs during the mitotic cycle in mammalian cells. *J. Biol. Chem.* **279**, 13721–13728 (2004).
19. Johannes, G. & Sarnow, P. Cap-independent polysomal association of natural mRNAs encoding c-myc, BiP, and eIF4G conferred by internal ribosome entry sites. *RNA* **4**, 1500–1513 (1998).
20. Krishnamoorthy, T., Pavitt, G.D., Zhang, F., Dever, T.E. & Hinnebusch, A.G. Tight binding of the phosphorylated  $\alpha$  subunit of initiation factor 2 (eIF2 $\alpha$ ) to the regulatory subunits of guanine nucleotide exchange factor eIF2B is required for inhibition of translation initiation. *Mol. Cell. Biol.* **21**, 5018–5030 (2001).
21. Stetson, D.B., Mohrs, M., Mallet-Designe, V., Teyton, L. & Locksley, R.M. Rapid expansion and IL-4 expression by Leishmania-specific naive helper T cells in vivo. *Immunity* **17**, 191–200 (2002).
22. Munn, D.H. *et al.* GCN2 kinase in T cells mediates proliferative arrest and energy induction in response to indoleamine 2,3-dioxygenase. *Immunity* **22**, 633–642 (2005).
23. Dey, M. *et al.* PKR and GCN2 kinases and guanine nucleotide exchange factor eukaryotic translation initiation factor 2B (eIF2B) recognize overlapping surfaces on eIF2 $\alpha$ . *Mol. Cell. Biol.* **25**, 3063–3075 (2005).
24. Bertolotti, A. & Ron, D. Alterations in an IRE1-RNA complex in the mammalian unfolded protein response. *J. Cell Sci.* **114**, 3207–3212 (2001).
25. Novoa, I., Zeng, H., Harding, H.P. & Ron, D. Feedback inhibition of the unfolded protein response by GADD34-mediated dephosphorylation of eIF2 $\alpha$ . *J. Cell Biol.* **153**, 1011–1022 (2001).
26. Ma, Y. & Hendershot, L.M. Herp is dually regulated by both the ER stress-specific branch of the UPR and by a branch that is shared with other cellular stress pathways. *J. Biol. Chem.* **279**, 13792–13799 (2004).
27. Vatter, K.M. & Wek, R.C. Reinitiation involving upstream ORFs regulates ATF4 mRNA translation in mammalian cells. *Proc. Natl. Acad. Sci. USA* **101**, 11269–11274 (2004).
28. Hellen, C.U. & Sarnow, P. Internal ribosome entry sites in eukaryotic mRNA molecules. *Genes Dev.* **15**, 1593–1612 (2001).
29. Marth, J.D., Overell, R.W., Meier, K.E., Krebs, E.G. & Perlmutter, R.M. Translational activation of the Ick proto-oncogene. *Nature* **332**, 171–173 (1988).
30. Blais, J.D. *et al.* Activating transcription factor 4 is translationally regulated by hypoxic stress. *Mol. Cell. Biol.* **24**, 7469–7482 (2004).
31. Kedersha, N.L., Gupta, M., Li, W., Miller, I. & Anderson, P. RNA-binding proteins TIA-1 and TIAR link the phosphorylation of eIF-2 $\alpha$  to the assembly of mammalian stress granules. *J. Cell Biol.* **147**, 1431–1442 (1999).
32. Kimball, S.R., Horetsky, R.L., Ron, D., Jefferson, L.S. & Harding, H.P. Mammalian stress granules represent sites of accumulation of stalled translation initiation complexes. *Am. J. Physiol. Cell Physiol.* **284**, C273–C284 (2003).
33. Kedersha, N. *et al.* Dynamic shuttling of TIA-1 accompanies the recruitment of mRNA to mammalian stress granules. *J. Cell Biol.* **151**, 1257–1268 (2000).
34. Boyce, M. *et al.* A selective inhibitor of eIF2 $\alpha$  dephosphorylation protects cells from ER stress. *Science* **307**, 935–939 (2005).
35. Johannes, G., Carter, M.S., Eisen, M.B., Brown, P.O. & Sarnow, P. Identification of eukaryotic mRNAs that are translated at reduced cap binding complex eIF4F concentrations using a cDNA microarray. *Proc. Natl. Acad. Sci. USA* **96**, 13118–13123 (1999).
36. Calton, M. *et al.* IRE1 couples endoplasmic reticulum load to secretory capacity by processing the XBP-1 mRNA. *Nature* **415**, 92–96 (2002).
37. Kuhn, K.M., DeRisi, J.L., Brown, P.O. & Sarnow, P. Global and specific translational regulation in the genomic response of *Saccharomyces cerevisiae* to a rapid transfer from a fermentable to a nonfermentable carbon source. *Mol. Cell. Biol.* **21**, 916–927 (2001).
38. Fernandez, J. *et al.* Ribosome stalling regulates IRES-mediated translation in eukaryotes, a parallel to prokaryotic attenuation. *Mol. Cell* **17**, 405–416 (2005).
39. Deng, J. *et al.* Translational repression mediates activation of nuclear factor  $\kappa$ B by phosphorylated translation initiation factor 2. *Mol. Cell. Biol.* **24**, 10161–10168 (2004).
40. Teixeira, D., Sheth, U., Valencia-Sanchez, M.A., Brengues, M. & Parker, R. Processing bodies require RNA for assembly and contain nontranslating mRNAs. *RNA* **11**, 371–382 (2005).
41. Anderson, P. & Kedersha, N. Stressful initiations. *J. Cell Sci.* **115**, 3227–3234 (2002).
42. Ingelfinger, D., Arndt-Jovin, D.J., Luhrmann, R. & Achsel, T. The human LSM1-7 proteins colocalize with the mRNA-degrading enzymes Dcp1/2 and Xrn1 in distinct cytoplasmic foci. *RNA* **8**, 1489–1501 (2002).
43. Reimold, A.M. *et al.* Plasma cell differentiation requires the transcription factor XBP-1. *Nature* **412**, 300–307 (2001).
44. Sawada, S., Scarborough, J.D., Killeen, N. & Littman, D.R. A lineage-specific transcriptional silencer regulates CD4 gene expression during T lymphocyte development. *Cell* **77**, 917–929 (1994).
45. Voehringer, D., Shinkai, K. & Locksley, R.M. Type 2 immunity reflects orchestrated recruitment of cells committed to IL-4 production. *Immunity* **20**, 267–277 (2004).
46. Ranganath, S. *et al.* GATA-3-dependent enhancer activity in IL-4 gene regulation. *J. Immunol.* **161**, 3822–3826 (1998).
47. Fowell, D.J. *et al.* Impaired NFATc translocation and failure of Th2 development in Itk-deficient CD4<sup>+</sup> T cells. *Immunity* **11**, 399–409 (1999).